

# Extraction of $P_{11}$ Resonance from $\pi N$ Data and Its Stability

S. X. Nakamura<sup>1,†</sup>, H. Kamano<sup>1</sup>, T.-S. H. Lee<sup>1,2</sup> and T. Sato<sup>1,3</sup>

<sup>1</sup> Excited Baryon Analysis Center (EBAC), Thomas Jefferson National Accelerator Facility, Newport News, Virginia 23606, USA

<sup>2</sup> Physics Division, Argonne National Laboratory, Argonne, Illinois 60439, USA

<sup>3</sup> Department of Physics, Osaka University, Toyonaka, Osaka 560-0043, Japan

E-mail: <sup>†</sup>satoshi@jlab.org

**Abstract.** An important question about resonance extraction is how much resonance poles and residues extracted from data depend on a model used for the extraction, and on the precision of data. We address this question with the dynamical coupled-channel (DCC) model developed in Excited Baryon Analysis Center (EBAC) at JLab. We focus on the  $P_{11}$   $\pi N$  scattering. We examine the model-dependence of the poles by varying parameters to a large extent within the EBAC-DCC model. We find that two poles associated with the Roper resonance are fairly stable against the variation. We also develop a model with a bare nucleon, thereby examining the stability of the Roper poles against different analytic structure of the  $P_{11}$  amplitude below  $\pi N$  threshold. We again find a good stability of the Roper poles.

## 1. Introduction

Extraction of  $N^*$  information, such as pole positions and vertex form factors, is an important task in hadron physics. This is because they are necessary information to address a question whether we can understand baryon resonances within QCD. In order to extract the  $N^*$  information, first, one needs to construct a reaction model through a comprehensive analysis of data. Then, pole positions and vertex form factors are extracted from the model with the use of the analytic continuation. Therefore, the  $N^*$  information extracted in this manner is inevitably model-dependent. There are several different approaches to extract the  $N^*$  information. Although almost all 4-stars nucleon resonances listed by Particle Data Group (PDG) are found in all approaches, existence of some  $N^*$  states, in particular those in the higher mass region, is controversial. Thus, commonly asked questions are how much model-dependent the extracted resonance parameters are, and how precise data have to be for a stable resonance extraction. These are the questions we would like to address in this work[1], within a dynamical coupled-channels model (EBAC-DCC) [2]. We focus on the  $\pi N$   $P_{11}$  partial wave and the stability of its pole positions, particularly those corresponding to the Roper resonance. In the region near Roper  $N(1440)$ , two poles close to the  $\pi\Delta$  threshold were found in our recent extraction [3] from the model obtained by the fit to  $\pi N \rightarrow \pi N$  scattering data (JLMS) [4].

while only one pole in the similar energy region was reported in some other analyses. We examine the stability of this two-pole structure against the following variation, keeping a good reproduction of SAID single-energy (SAID-SES) solution [5] unless otherwise stated:

- Large variation of the parameters of the meson-exchange mechanisms as well as bare  $N^*$  parameters of the EBAC-DCC model.
- Inclusion of a bare nucleon state: The analytic structure of this model is rather different from the original EBAC-DCC model, in particular in the region near the nucleon pole [6], .
- Fit to the solution based on the Carnegie-Mellon University-Berkeley model (CMB) [7] which has rather different behavior from SAID-SES for higher  $W$ .

## 2. Dynamical coupled-channels models and analytic continuation

In this section, we briefly describe dynamical coupled-channels model used in this work, followed by a brief explanation for the analytic continuation used to extract poles from the model.

### 2.1. EBAC-DCC model

The EBAC-DCC model contains  $\pi N$ ,  $\eta N$  and  $\pi\pi N$  channels and the  $\pi\pi N$  channel has  $\pi\Delta$ ,  $\rho N$  and  $\sigma N$  components. These meson-baryon (MB) channels are connected with each other by meson-baryon interactions ( $v_{MB,M'B'}$ ), or excited to bare  $N^*$  states by vertex interactions ( $\Gamma_{MB\leftrightarrow N^*}$ ). With these interactions, the partial-wave amplitude for the  $M(\vec{k}) + B(-\vec{k}) \rightarrow M'(\vec{k}') + B'(-\vec{k}')$  reaction can be written by the following form:

$$T_{MB,M'B'}(k, k', E) = t_{MB,M'B'}(k, k', E) + t_{MB,M'B'}^R(k, k', E), \quad (1)$$

where the first term is obtained by solving the following coupled-channels Lippmann-Schwinger equation:

$$t_{MB,M'B'}(k, k', E) = v_{MB,M'B'}(k, k') + \sum_{M''B''} \int_{C_{M''B''}} q^2 dq v_{MB,M''B''}(k, q) G_{M''B''}(q, E) t_{M''B'',M'B'}(q, k', E). \quad (2)$$

Here  $C_{MB}$  is the integration contour in the complex- $q$  plane used for the channel  $MB$ . The second term of Eq. (1) is associated with the bare  $N^*$  states, and given by

$$t_{MB,M'B'}^R(k, k', E) = \sum_{i,j} \bar{\Gamma}_{MB\rightarrow N_i^*}(k, E) [D(E)]_{i,j} \bar{\Gamma}_{N_j^*\rightarrow M'B'}(k', E), \quad (3)$$

where the dressed vertex function  $\bar{\Gamma}_{N_j^*\rightarrow M'B'}(k, E)$  is calculated by convoluting the bare vertex  $\Gamma_{N_j^*\rightarrow M'B'}(k)$  with the amplitudes  $t_{MB,M'B'}(k, k', E)$ . The inverse of the propagator of dressed  $N^*$  states in Eq. (3) is

$$[D^{-1}(E)]_{i,j} = (E - m_{N_i^*}^0) \delta_{i,j} - \Sigma_{i,j}(E), \quad (4)$$

where  $m_{N_i^*}^0$  is the bare mass of the  $i$ -th  $N^*$  state, and the  $N^*$  self-energy is defined by

$$\Sigma_{i,j}(E) = \sum_{MB} \int_{C_{MB}} q^2 dq \bar{\Gamma}_{N_j^*\rightarrow MB}(q, E) G_{MB}(q, E) \Gamma_{MB\rightarrow N_i^*}(q, E). \quad (5)$$

Defining  $E_\alpha(k) = [m_\alpha^2 + k^2]^{1/2}$  with  $m_\alpha$  being the mass of particle  $\alpha$ , the meson-baryon propagators in the above equations are:  $G_{MB}(k, E) = 1/[E - E_M(k) - E_B(k) + i\epsilon]$  for the stable  $\pi N$  and  $\eta N$  channels, and  $G_{MB}(k, E) = 1/[E - E_M(k) - E_B(k) - \Sigma_{MB}(k, E)]$  for the unstable  $\pi\Delta$ ,  $\rho N$ , and  $\sigma N$  channels. The self energy  $\Sigma_{MB}(k, E)$  is calculated from a vertex function defining the decay of the considered unstable particle in the presence of a spectator  $\pi$  or  $N$  with momentum  $k$ . For example, we have for the  $\pi\Delta$  state,

$$\Sigma_{\pi\Delta}(k, E) = \frac{m_\Delta}{E_\Delta(k)} \int_{C_3} q^2 dq \frac{M_{\pi N}(q)}{[M_{\pi N}^2(q) + k^2]^{1/2}} \frac{|f_{\Delta\rightarrow\pi N}(q)|^2}{E - E_\pi(k) - [M_{\pi N}^2(q) + k^2]^{1/2} + i\epsilon}, \quad (6)$$

where  $M_{\pi N}(q) = E_\pi(q) + E_N(q)$  and  $f_{\Delta\rightarrow\pi N}(q)$  defines the decay of the  $\Delta \rightarrow \pi N$  in the rest frame of  $\Delta$ ,  $C_3$  is the corresponding integration contour in the complex- $q$  plane.

## 2.2. Bare nucleon model

To examine further the model dependence of resonance extractions, it is useful to also perform analysis using models with a bare nucleon, as developed in Ref. [8]. Within the formulation given in Sec. 2.1, such a model can be obtained by adding a bare nucleon ( $N_0$ ) state with mass  $m_N^0$  and  $N_0 \rightarrow MB$  vertices and removing the direct  $MB \rightarrow N \rightarrow M'B'$  in the meson-baryon interactions  $v_{MB,M'B'}$ . All numerical procedures for this model are identical to that used for the EBAC-DCC model, except that the resulting amplitude must satisfy the nucleon pole condition:

$$t_{\pi N, \pi N}^R(k \rightarrow k_{\text{on}}, k \rightarrow k_{\text{on}}, E \rightarrow m_N) = -\frac{[F_{\pi NN}(k_{\text{on}})]^2}{E - m_N^0 - \tilde{\Sigma}(m_N)}. \quad (7)$$

with

$$m_N = m_N^0 + \tilde{\Sigma}(m_N) \quad \text{and} \quad F_{\pi NN}(k_{\text{on}}) = F_{\pi NN}^{\text{phys.}}(k_{\text{on}}). \quad (8)$$

Here we have used the on-shell momentum defined by  $E = \sqrt{m_N^2 + k_{\text{on}}^2} + \sqrt{m_\pi^2 + k_{\text{on}}^2}$  ( $\text{Im}[k_{\text{on}}] > 0$ ). Also,  $\tilde{\Sigma}(m_N)$  is the self-energy for the nucleon. More details for the calculational procedure following Afnan and Pearce are found in Refs. [1, 8].

## 2.3. Analytic continuation

Once a fit is obtained, we then apply the method of analytic continuation to find resonance poles. The procedures for performing this numerical task have been discussed in Ref. [3, 9]. To search for resonance poles, as discussed in the above references, the contours  $C_{MB}$  and  $C_3$  must be chosen appropriately to solve Eqs. (2)-(6) for  $E$  on the various possible sheets of the Riemann surface. We only look for poles which are close to the physical region and have effects on the  $\pi N$  scattering observables. All of these poles are on the unphysical sheet of the  $\pi N$  channel, but could be on either unphysical ( $u$ ) or physical ( $p$ ) sheets of other channels considered in this analysis. We will indicate the sheets where the identified poles are located by  $(s_{\pi N}, s_{\eta N}, s_{\pi\pi N}, s_{\pi\Delta}, s_{\rho N}, s_{\sigma N})$ , where  $s_{MB}$  and  $s_{\pi\pi N}$  can be  $u$  or  $p$ . The errors of the resonance parameters are estimated by using all values obtained in all fits we have performed.

## 3. Results

Now we show our numerical results to examine the stability of the  $P_{11}$  poles. First of all, we show  $P_{11}$  amplitudes from JLMS and SAID-EDS (energy-dependent)[5] compared with SAID-SES in Fig. 1. In Table 1, the pole positions from JLMS and SAID-EDS as well as  $\chi^2$  per data point ( $\chi_{pd}^2$ ) are given. In the following subsections, we present results from various fits by varying the dynamical content of the EBAC-DCC model, using a model with a bare nucleon, and using different empirical amplitude for the fit.

### 3.1. $2N^*-3p$ and $2N^*-4p$ fits

We varied both the parameters for the meson-baryon interactions ( $v_{MB,M'B'}$ ) and parameters associated with bare  $N^*$  states ( $m_{N^*}^0, \Gamma_{N^* \leftrightarrow MB}$ ). The obtained meson-baryon interactions are quite different from those of JLMS. We obtained several fits which are different in how the oscillatory behavior of SAID-SES amplitude for higher  $W$  is fitted. The results from the  $2N^*-3p$  (dotted curves) and  $2N^*-4p$  (dashed curves) fits are compared with the JLMS fit (solid curves) in Fig. 2. The resulting resonance poles are listed in the 3th and 4th rows of Table 1. Here we see again the first two poles near the  $\pi\Delta$  threshold from both fits agree well with the JLMS fit. This seems to further support the conjecture that these two poles are mainly sensitive to the data below  $W \sim 1.5$  GeV where the SAID-SES has rather small errors. However, the  $2N^*-4p$  fit has one more pole at  $M_R = 1630 - i45$  MeV. This is perhaps related to its oscillating structure

**Table 1.** The resonance pole positions  $M_R$  for  $P_{11}$  [listed as  $(\text{Re}M_R, -\text{Im}M_R)$  in the unit of MeV] extracted from various parameter sets. The location of the pole is specified by, e.g.,  $(s_{\pi N}, s_{\eta N}, s_{\pi\pi N}, s_{\pi\Delta}, s_{\rho N}, s_{\sigma N}) = (upuupp)$ , where  $p$  and  $u$  denote the physical and unphysical sheets for a given reaction channel, respectively.  $\chi_{pd}^2$  is  $\chi^2$  per data point.

Model	$upuupp$	$upuppp$	$uuuupp$	$uuuuup$	$\chi_{pd}^2$
SAID-EDS	(1359, 81)	(1388, 83)	—	—	2.94
JLMS	(1357, 76)	(1364, 105)	—	(1820, 248)	3.55
$2N^*-3p$	(1368, 82)	(1375, 110)	—	(1810, 82)	3.28
$2N^*-4p$	(1372, 80)	(1385, 114)	(1636, 67)	(1960, 215)	3.36
$2N^*-4p\text{-CMB}$	(1379, 89)	(1386, 109)	(1613, 42)	(1913, 324)	4.91
$1N_01N^*-3p$	(1363, 81)	(1377, 128)	—	(1764, 137)	2.51

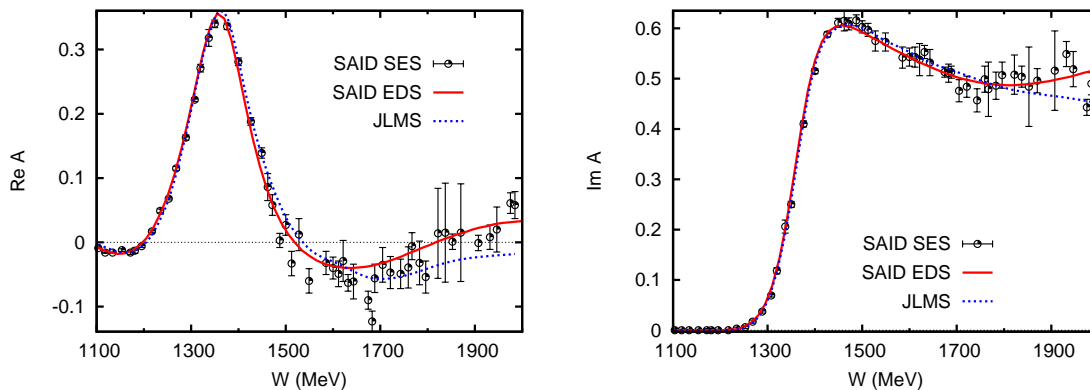


**Figure 1.** The real (left) and imaginary (right) parts of the on-shell  $P_{11}$  amplitudes as a function of the  $\pi N$  invariant mass  $W$  (MeV). The solid curves are from the JLMS fit; the open circles are the SAID-EDS [5].  $A$  is unitless in the convention of Ref. [5].

near  $W \sim 1.6$  GeV (dashed curves), as shown in the Figs. 2. On the other hand, this resonance pole could be fictitious since the fit  $2N^*-3p$  (dotted curve) with only three poles are equally acceptable within the fluctuating experimental errors. Our result suggests that it is important to have more accurate data in the high  $W$  region for a high precision resonance extraction.

### 3.2. $1N_01N^*-3p$

Here we show our results obtained with the bare nucleon model, and then address the question whether difference in the analytic structure of the  $\pi N$  amplitude below  $\pi N$  threshold strongly affects the resonance extractions. The bare nucleon model is fitted to SAID-SES, and at the same time, to the nucleon pole conditions Eq. (8). Meanwhile, the original EBAC-DCC model has different singular structure below the  $\pi N$  threshold. The question is whether such differences can lead to very different resonance poles. Our fit of the bare nucleon model is shown in Fig. 3 and compared with SAID-SES and JLMS. We see that the two fits agree very well below  $W = 1.5$  GeV, while their differences are significant in the high  $W$  region. The corresponding resonance

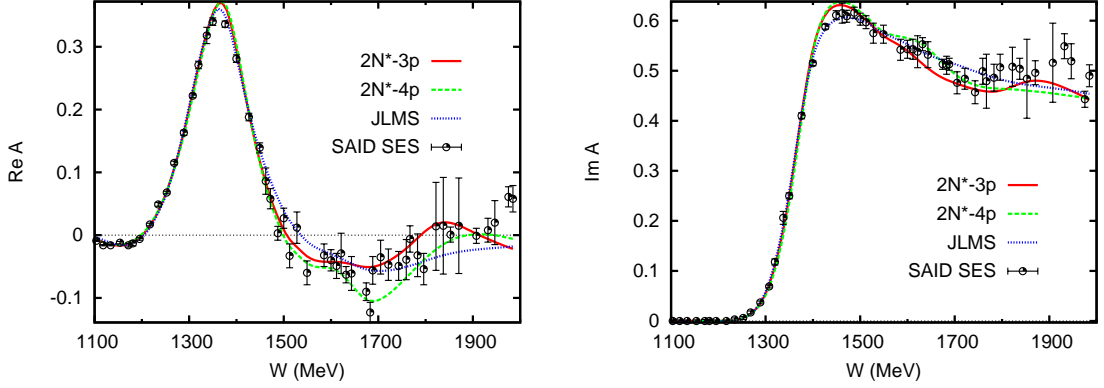


**Figure 2.** The real (left panel) and imaginary (right panel) parts of the  $P_{11}$  amplitudes.

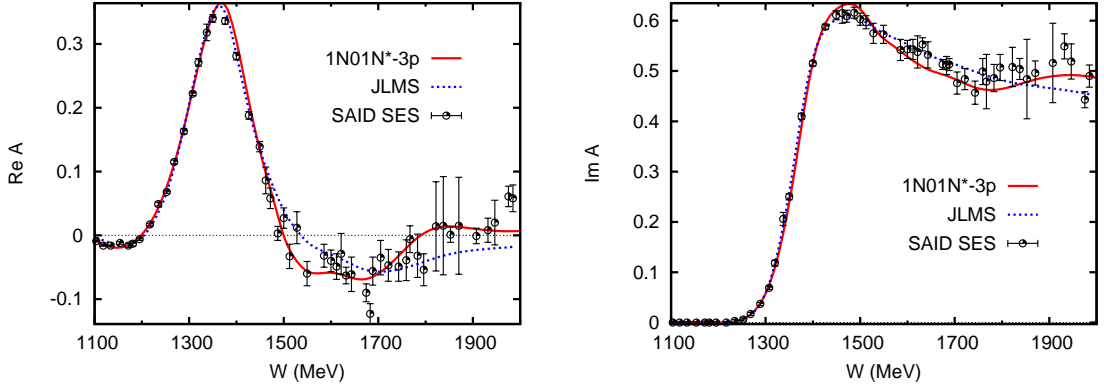


**Figure 3.** The real (left panel) and imaginary (right panel) parts of the  $P_{11}$  amplitudes.

poles are given in Table 1. We also see here that the first two poles near the  $\pi\Delta$  threshold are close to those of JLMS. Our results seem to indicate that these two poles are rather insensitive to the analytic structure of the amplitude in the region below  $\pi N$  threshold, and are mainly determined by the data in the region  $m_N + m_\pi \leq W \leq 1.6$  GeV.

### 3.3. $2N^*-4p$ -CMB fit

To further explore the dependence of the resonance poles on the data, we consider a solution from CMB collaboration [7]. This solution differs significantly from the SAID-SES mainly at  $W > 1.55$  GeV. For our present purpose of investigating the stability of the lowest two poles near the  $\pi\Delta$  threshold, we fit the data which is obtained from replacing SAID-SES in the high  $W > 1.55$  GeV region by the CMB solution. The results (dashed curves) from this fit are compared with JLMS in Fig. 4. We see that the CMB solution has oscillating behavior near  $W \sim 1.6$  GeV and this could be the reason why the fit has an addition pole near  $W \sim 1.6$  GeV, as seen in 5th row of Table 1. The large differences from JLMS at high  $W$  make the poles near  $W \sim 1.9$  GeV very different; in particular their imaginary parts. On the other hand, their lowest two poles near the  $\pi\Delta$  threshold are close to other fits discussed so far. This again supports the above observation that these two poles are determined only by the data below  $W < 1.5$  GeV which are reproduced very well in all fits.

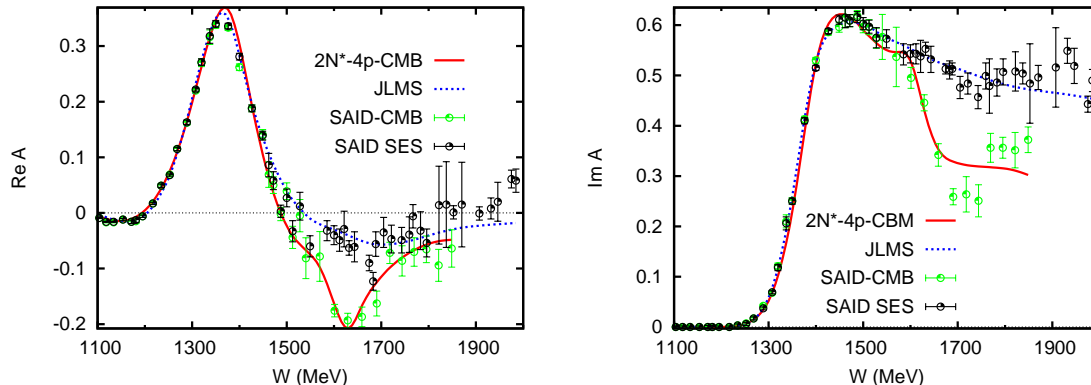


**Figure 4.** The real (left) and imaginary (right) parts of the  $P_{11}$  amplitudes.

#### 4. Conclusion

We have examined the stability of the two-pole structure of the Roper resonance. We showed that two resonance poles near the  $\pi\Delta$  threshold are stable against large variations of parameters of meson-exchange mechanisms within EBAC-DCC model [2]. This two-pole structure is also obtained in an analysis based on a model with the bare nucleon state. Our results indicate that the extraction of  $P_{11}$  resonances is insensitive to the analytic structure of the amplitude in the region below  $\pi N$  threshold. We have also fitted to the old CMB amplitude, which is rather different from SAID-SES for  $W \geq 1.5$  GeV, and still found that the Roper two poles are stable.

#### Acknowledgments

This work is supported by the U.S. Department of Energy, Office of Nuclear Physics Division, under Contract No. DE-AC02-06CH11357, and Contract No. DE-AC05-06OR23177 under which Jefferson Science Associates operates Jefferson Lab, and by the Japan Society for the Promotion of Science, Grant-in-Aid for Scientific Research(C) 20540270. This research used resources of the National Energy Research Scientific Computing Center, which is supported by the Office of Science of the U.S. Department of Energy under Contract No. DE-AC02-05CH11231.

#### References

- [1] Kamano H, Nakamura S X, Lee T-S H, Matsuyama A and Sato T 2010 *Phys. Rev. C* **81** 065207
- [2] Matsuyama A, Sato T and Lee T-S H 2007 *Phys. Rep.* **439** 193
- [3] Suzuki N, Juliá-Díaz B, Kamano H, Lee T-S H, Matsuyama A and Sato T 2010 *Phys. Rev. Lett.* **104** 042302
- [4] Juliá-Díaz B, Lee T-S H, Matsuyama A and Sato T, 2007 *Phys. Rev. C* **76** 065201
- [5] Arndt R A, Briscoe W J, Strakovsky I I and Workman R L, 2006 *Phys. Rev. C* **74** 045205
- [6] Juliá-Díaz B, Kamano H, Lee T-S H, Matsuyama A, Sato T and Suzuki N 2009 *Chin. J. Phys.* **47** 142
- [7] Cutkosky R E and Wang S 1990 *Phys. Rev. D* **42** 235
- [8] Pearce B C and Afnan I R 1986 *Phys. Rev. C* **34** 991; 1989 *Phys. Rev. C* **40** 220
- [9] Suzuki N, Sato T and Lee T-S H 2009 *Phys. Rev. C* **79**, 025205 (2009); arXiv:1006.2196[nucl-th].